PHYSICAL REVIEW B, VOLUME 64, 241403(R)

Locked twist in multiwalled carbon-nanotube ribbons

Min-Feng Yu,* Mark J. Dyer, and Jian Chen
Zyvex Corporation, Advanced Technologies Group, 1321 North Plano Road, Richardson, Texas 75081

Dong Qian, Wing Kam Liu, and Rodney S. Ruoff†
Northwestern University, Department of Mechanical Engineering, Evanston, Illinois 60208
(Received 24 September 2001; published 29 November 2001)

Twisted multiwalled carbon-nanotube (MWCNT) ribbons were observed with transmission electron microscopy. Particularly one cantilevered MWCNT ribbon had a twist present in the freestanding segment. An energetics analysis was presented supporting the hypothesis that twists in MWCNT ribbons are stabilized through more favorable atomic registry between neighboring layers in the twisted state.

DOI: 10.1103/PhysRevB.64.241403 PACS number(s): 61.48.+c, 68.37.Lp

Carbon nanotubes (CNTs) are valuable materials for nanoscale studies of electronics and mechanics. Many predicted atomistic and quantum effects have been observed experimentally with CNTs. Examples include the Van Hove singularities in the band structure of one-dimensional materials,[1,2] ballistic electron transport at room temperature,[3] the Aharonov-Bohm effect,[4,5] and near frictionless sliding with attendant surface tension effect between neighboring carbon-nanotube shells.[6–8]

Various molecular or atomistic interactions, normally negligible in macroscopic systems, become critical factors in the study of the mechanics of nanoscale systems. An example is the interaction between commensurate or incommensurate crystalline surfaces. This is illustrated by the near frictionless sliding between nested and neighboring shells inside MWCNTs (Refs. 6 and 8) and the sliding (incommensurate) vs. rolling (commensurate) of MWCNTs on a graphite surface.[9,10]

Fully collapsed MWCNTs (MWCNT ribbons) have been observed by transmission electron microscopy (TEM) (Ref. 11) and by atomic force microscopy (AFM).[12] Experimental observations are in accord with a simple energetics analysis showing that particular CNT structures favor full collapse or are metastable once collapsed. Such deformation either minimizes the free energy of the CNT (Refs. 11 and 13) or provides a local minimum with a barrier large enough to maintain the collapsed state. In the analysis of mechanical strain and surface energy contributions, the effect of atomic registry between graphitic lattices has been ignored so far. Twists in collapsed MWCNTs (Refs. 11 and 12) and collapsed large diameter single wall CNTs (Ref. 14) on surfaces or suspended across supports have also been observed, but no explanation for their existence has yet been provided. It has recently been proposed that the competition between curvature elasticity and interlayer adhesion is the cause for the coil formation of MWCNTs during growth;[15] and that intertube interactions based on atomic lattice registry between single wall CNTs of different helicity are responsible for the recently observed twisted single wall CNT ropes.[16,17]

We present here observations of a freestanding (anchored only at one end) twisted MWCNT ribbon, and other suspended and periodically twisted MWCNT ribbons, obtained by TEM. We propose that the achievement of more favorable interlayer atomic registry between neighboring layers of the collapsed innermost MWCNT shell in the twisted state is responsible for the presence of twists along the MWCNT ribbon.

Arc-grown MWCNT material purified by oxidation in air was examined in the experiment. A dispersion in 2-butanone was prepared by bath sonication. TEM samples were prepared by placing a small droplet of the dispersion onto a formvar-free lacy carbon TEM grid and drying in air. A JEOL 2000FX transmission electron microscope operated at 120 KV was used for imaging.

We first discuss the observed MWCNT ribbon geometries, and then discuss a possible mechanism for twist formation in these ribbons. Figure 1(a) shows a twist (twist 1) along a *freestanding* MWCNT ribbon section and another twist in the same ribbon (twist 2) present in a section on the carbon support film, both indicated by arrows in the figure. The width of the flat part of the ribbon is 28 nm, the length of the freestanding section is 478 nm as measured from point A to point C, the length from point B to point C is 232 nm and from point B to point D is 471 nm. These distances demonstrate a periodic distance of ~470 nm between twists. Fringes along both edges of the ribbon can be resolved in the section just sticking out from the carbon support [Fig. 1(b) for the left edge and Fig. 1(c) for the right edge], which indicates that the ribbon is a collapsed 8-walled CNT. It was not possible to resolve the fringes along twist 1 due to vibration, or along twist 2, which resided on the surface of the grid carbon film and are obscured by it. Fringes along twists, or ribbon edges, typically were resolvable for ribbon sections supported at both ends by the lacy carbon grid. Figure 2(a) shows a 32 nm wide ribbon suspended across the hole in the lacy carbon TEM grid with two twists present. The distance between the twist nodes is 412 nm. Figures 2(b) and 2(c) show 10 resolved fringes for twist 1 and also for twist 2 [as marked in Fig. 2(a)]. Figure 2(d) shows five fringes along the left edge of the ribbon and Fig. 2(e) five fringes along the right edge of the ribbon imaged near the cross between the ribbon and the carbon support (top part) in Fig. 2(a). The ribbon thus has five fully collapsed nested shells, as evident from the observed five fringes along both ribbon edges and the observed ten fringes along the twists.

The presence of the twist in the *freestanding* CNT ribbon section shown in Fig. 1 excludes the CNT ribbon being con-

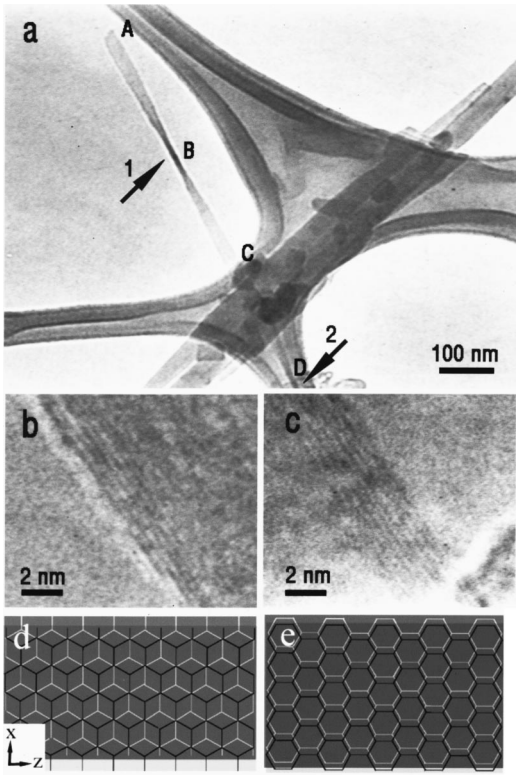

FIG. 1. A freestanding twisted MWCNT ribbon. (a) A TEM image of this ribbon anchored on one end by a carbon support film on a lacy carbon grid. Arrows point to the twists in the ribbon. (b) and (c) 8 resolved fringes along both edges of the ribbon imaged near the anchor point. (d) A schematic depicting the AB stacking between armchair CNT shells (the layer having brighter background and black lattices versus the layer having darker background and white lattices). The AB stacking can be achieved by just shifting the layer positions along the *x* direction that is perpendicular to the long axis of the MWCNT cylinder. (e) A schematic depicting the lattice alignment between the zigzag CNT shells by allowing the relative shifting of the layers along *x* direction. The AB stacking is not possible and only AA stacking or other stacking (as shown in the schematic) is possible.

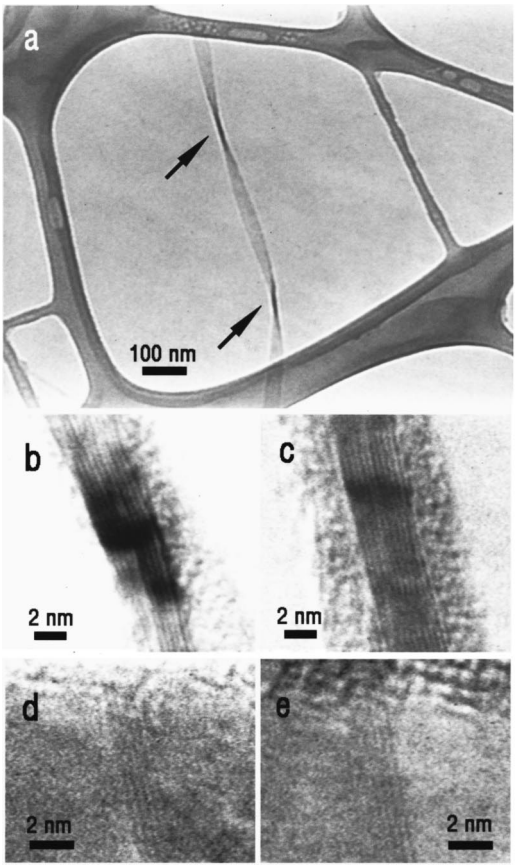

FIG. 2. A suspended twisted MWCNT ribbon. (a) A TEM image of this ribbon spanning a hole and supported at both sides by the carbon support film. Arrows indicate the twists. (b) and (c) TEM images of 10 resolved fringes at twist 1 and twist 2 in (a). (d) and (e) TEM images of 5 resolved fringes along the right edge (d) and the left edge (e) of the ribbon.

sidered simply as a homogenous elastic strip and treated only using general elastic mechanics, since a twisted elastic strip would automatically untwist once one end is free from external torsional stress. The static existence of the twist inside a TEM vacuum environment also excludes the dynamic injection of twists as observed in modeling string or strip dynamics in a liquid environment where force field fluctuations are constantly present.[18–20] It is difficult to map out the exact route the ribbon may have followed to form this twist in this freestanding ribbon. Ribbon twisting may have been triggered in the 2-butanone dispersion, which is the case for DNA or other long chain polymers in a liquid environment. However, we will not consider the dynamics of the twist formation in the MWCNT ribbon here, which of course is a very interesting topic in and of itself. Instead, we begin our analysis from the observation in experiment that a static twist is present in a freestanding ribbon, and then try to answer the immediate question: what holds this twist in place?

For the observed twist in Fig. 1 to remain in this freestanding CNT ribbon, internal torsional stress from the ribbon itself has to be present. Owing to the helical nature of CNT, one intriguing way to provide this internal stress is via the interlayer interactions that are dependent upon the type of interlayer atomic registry between surfaces of collapsed MWCNT shells. We provide below a simple model of the energetics that compares the energy cost of twist formation with the energy gain due to achieving more favorable interlayer atomic registry.

We first consider the energy gain due to the atomic registry-dependent interactions. Recently, a *registry-dependent graphitic potential* has been developed which accounts for the exponential atomic-core repulsion and the interlayer delocalization of π orbitals in addition to the normal two-body van der Waals attraction.[8] Based on this potential, the difference in the interlayer binding energy of the AA and the AB stacking configurations for two rigid graphitic layers spaced 0.344 nm apart shows the AB stacking to be 12 meV/atom more stable.[8] Typically, the collapse of a single CNT cylinder cannot result in perfect ''AB'' interlayer stacking. The only exception is for fully collapsed (n,n) ''armchair'' single wall CNTs, where perfect AB interlayer stacking is possible [as shown in Fig. 1(d)] by adjusting the relative

position of layers along the direction (x axis) perpendicular to the long axis (z axis) of the CNT. The adjustment between layers of a collapsed CNT shell along the x axis is obviously easier (it does not involve extra C-C bond deformation) than sliding along other directions, considering the boundary conditions for a collapsed cylinder.

As mentioned, for other types of CNT than armchair, simple translation adjustment along the x axis cannot result in AB interlayer stacking. For example, the collapse of a $(n,0)$ ''zigzag'' CNT shell can only result in AA stacking or by relative sliding of the layers along the x axis, other types of stacking [as shown in Fig. 1(e)]. For these collapsed CNT shells, there is a ''frustration effect'' where imperfect registry produces internal interlayer in-plane stress that can contribute to the mechanical deformation of the ribbon, for example, generating or maintaining a twist. Achieving high commensurance in atomic registry would be counterbalanced by intralayer C-C bond length changes.

The similar analysis for the external shells of a collapsed MWCNT would be different. Here only the interactions between the shells, not between the layers of the same collapsed shell which is the case for the innermost shell, are meaningful, since the distance between the layers of the same collapsed external shell increases in the multiple of interlayer distance, 0.34 nm, and the van der Waals interactions between these layers diminish sharply and can be ignored. Another point for the external shells different from the innermost shell is that external shells are allowed to slide along both x and z direction relative to each other without introducing in-plane stress, so achieving higher commensurance between the outer shells is relatively easy energetically.

In the following model, the maximum interlayer energy difference is assumed to be the binding energy difference E_b (12 meV/atom, Ref. 8) between the AA and AB stackings for the graphene layers in the MWCNT ribbon. The change in the binding energy when twisted for a MWCNT ribbon is defined as ϕ_1. The elastic energy that is necessary to achieve a twisted configuration is defined as ϕ_2. If $\phi_1 > \phi_2$, then the twisted configuration is favorable, otherwise, the MWCNT will only undergo ''sliding'' with no or little twist, or, if twisted, the twist is metastable.

We consider an m-walled MWCNT ribbon having a width of w in nm. Upon considering the change in binding energy of the twisted state relative to the straight, flat ribbon state, only the innermost shell is considered. So, $\phi_1 = \lambda E_b(w-2md)l/s$ meV, where λ represents the change of the degree of commensurance between the top and bottom layers of the innermost MWCNT shell. The value of λ is between 0 (no interlayer stacking change) and 1 (changing the interlayer stacking from AA to AB stacking). Here, d is the graphene layer thickness, 0.34 nm (so the width of the flattened part of the collapsed innermost shell is approximately $w-2md$), l is the length of the ribbon, and s is the area occupied by one carbon atom in the graphene sheet, 0.026 nm^2.

It is also possible that the high curvature bulb formation in the twisted MWCNT has a preferred direction due to the hexagonal lattice structure of the graphene layer, which might contribute to the free energy of the system. However, in a separate calculation of the bending energy required for rolling a graphene sheet along different lattice directions, we found that the dependence is very minor, and is thus not included in our model.

We next consider the energy cost for the twist formation of the same collapsed MWCNT. The energy cost for the twist formation is modeled by considering the torsion of nested thin-walled pipes having rectangular cross sections. The thickness of each pipe is equal to the thickness of a graphene layer, d, 0.34 nm. Each pipe has a width $a=(w-2nd)$ and a height $b=(2m-2n-1)d$, where w is the measured width of the observed ribbon in TEM and n is the designated number for each graphene pipe, beginning from 0 for the outermost shell. The torsional elastic energy E_n of a thin-walled pipe can be calculated as[21]

$$E_n = \frac{1}{2}\int C\tau^2 dl \tag{1}$$

with C the torsional rigidity of the pipe and τ is the torsion angle, which is the angle of rotation per unit length of the twisted beam. $C=2\mu d(ab)^2/(a+b)$, where μ is the appropriate elastic modulus. (For a solid beam as considered in Ref. 16, μ is the shear modulus in its thin beam approximation.) So

$$E_n = \mu\tau^2 d^3 l(w-2nd)^2(2m-2n-1)^2/(w+2md-4nd-d) \tag{2}$$

and

$$\phi_2 = \sum_{n=0}^{m-1} E_n . \tag{3}$$

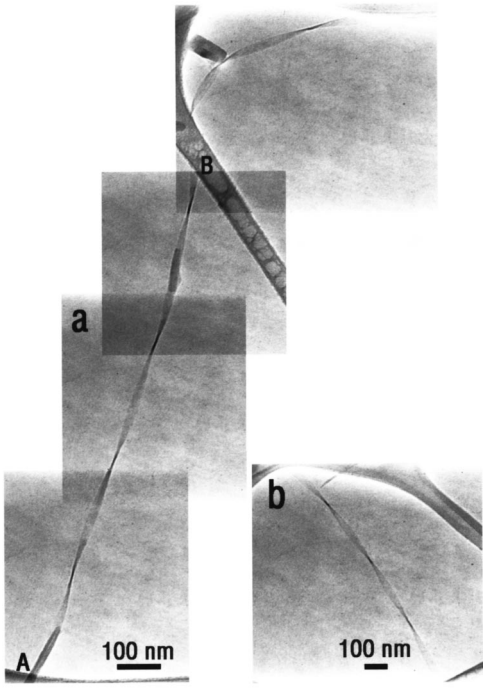

FIG. 3. (a) A TEM image of a long, periodically twisted MWCNT ribbon. (Notice the MWCNT ribbon begins from the end of this MWCNT.) (b) A TEM image of another periodically twisted MWCNT ribbon.

Due to the significant anisotropic mechanical properties of the layered structure of the CNT ribbon, the choice of the elastic modulus appropriate for the calculation of the torsional energy for the ribbon is not trivial. Instead, we consider each thin-walled graphite pipe to be homogenous and have an elastic modulus value of the bulk modulus of graphite, so $\mu = E/2(1+\gamma)$, where E is the Young's Modulus, 1 TPa and γ, the Poisson's ratio, 0.2, of graphite, thus $\mu = 420\,\mathrm{GPa}$.

For the twisted ribbon in Fig. 1, the stabilization energy ϕ_1 per unit length is calculated to be 10.4λ eV/nm. For the same ribbon, the torsion angle τ is equal to $\pi/470$ (nm^{-1}), and the calculated torsional elastic energy ϕ_2 per unit length is 73.5 eV/nm. This calculation suggests that the energy cost for the twist formation of this particular CNT ribbon can be partially compensated by achieving greater atomic registry. The observation of the existence of this freestanding twist in the ribbon thus suggests that an energy barrier might exist to keep the twisted ribbon from untwisting. The twisted structure of CNT ribbon is thus probably metastable. More complex theoretical treatment is called for to calculate this energy barrier. For the twisted ribbon in Fig. 2, which is supported by the carbon film on both sides, ϕ_1 is calculated to be 13.2λ eV/nm, and ϕ_2, 28.8 eV/nm.

The periodicity of twists in CNT ribbons is clearly shown in Fig. 3. The long, twisted CNT ribbon (20 nm in width) shown in Fig. 3(a) has an average period of 293 nm for the three twists spanning the hole between point A and point B. The twisted CNT ribbon (34 nm in width) shown in Fig. 3(b) has an average period of 312 nm. Long and untwisted flat ribbons were also found on the TEM grid occasionally, which might indicate either a better atomic registry between the layers (for the untwisted geometry) in these ribbons based on our above analysis or that they were never subjected to external torsional stress and thus never quenched into a metastable twisted state.

The subject of the elasticity of filament or strips has attracted recent attention, as it is closely related to the dynamics of various biopolymers, such as DNA, and potentially to their function. Mechanical models for the dynamics of real biological chain polymers have typically not included structural details at the molecular level. Recent success in synthesizing structurally perfect semiconducting oxides ''nanoribbons'' may contribute to research on the mechanics of nanosized ribbons.[22] Our observation of twisted CNT ribbons (in the absence of any external torsion) suggests that atomic or molecular level interactions could play the deciding role in the final structure. Indeed, we propose that the achievement of more favorable interlayer registry can act as a driving force for large deformation of nanoscale specimens such as thin platelets and compliant nanotubes.

R.S.R. appreciates support from the NASA Langley Research Center Computational Materials: Nanotechnology Modeling and Simulation Program, and support to R.S.R., D.Q. and W.K.L. from the ONR (initially from NSF) Miniaturized Intelligent Sensors Program. We appreciate a critical reading of the manuscript by Thomas Powers.

*Email address: mfyu@zyvex.com

†Email address: r-ruoff@northwestern.edu

[1] J. W. G. Wildoer, L. C. Venema, A. G. Rinzier, R. E. Smalley, and C. Dekker, Nature (London) **391**, 59 (1998).

[2] P. Kim, T. W. Odom, J.-L. Huang, and C. M. Lieber, Phys. Rev. Lett. **82**, 1225 (1999).

[3] S. Frank, P. Poncharal, Z. L. Wang, and W. A. de Heer, Science **280**, 1744 (1998).

[4] H. Ajiki and T. Ando, Science **265**, 1850 (1994).

[5] A. Bachtold, C. Strunk, J.-P. Salvetat, J.-M. Bonard, and L. Forr *et al.*, Nature (London) **397**, 673 (1999).

[6] M.-F. Yu, B. I. Yakobson, and R. S. Ruoff, J. Phys. Chem. B **104**, 8764 (2000).

[7] J. Cummings and A. Zettl, Science **289**, 602 (2000).

[8] A. N. Kolmogorov and V. H. Crespi, Phys. Rev. Lett. **85**, 4727 (2000).

[9] M. R. Falvo, R. M. Taylor II, A. Hesler, V. Chi, and F. P. Brooks, Jr. *et al.*, Nature (London) **397**, 236 (1999).

[10] A. Buldum and J. P. Lu, Phys. Rev. Lett. **83**, 5050 (1999).

[11] N. G. Chopra, L. X. Benedict, V. H. Crespi, M. L. Cohen, and S. G. Louie *et al.*, Nature (London) **377**, 135 (1995).

[12] M.-F. Yu, T. Kowalewski, and R. S. Ruoff, Phys. Rev. Lett. **86**, 87 (2000).

[13] L. X. Benedict, N. G. Chopra, M. L. Cohen, A. Zettl, and S. G. Louie *et al.*, Chem. Phys. Lett. **286**, 490 (1998).

[14] C.-H. Kiang, W. A. Goddard III, R. Beyers, and D. S. Bethune, J. Phys. Chem. **100**, 3749 (1996).

[15] O.-Y. Zhong-can, Z.-B. Su, and C.-L. Wang, Phys. Rev. Lett. **78**, 4055 (1997).

[16] W. Clauss, D. J. Bergeron, and A. T. Johnson, Phys. Rev. B **58**, R4266 (1998).

[17] Y.-K. Kwon and D. Tomanek, Phys. Rev. Lett. **84**, 1483 (2000).

[18] R. E. Goldstein, T. R. Powers, and C. H. Wiggins, Phys. Rev. Lett. **80**, 5232 (1998).

[19] A. Goriely and P. Shipman, Phys. Rev. E **61**, 4508 (1999).

[20] R. Golestanian and T. B. Liverpool, Phys. Rev. E **62**, 5488 (2000).

[21] L. D. Landau and E. M. Lifshitz, *Theory of Elasticity* (Butterworth-Heinemann, Oxford, 1999).

[22] Z. W. Pan, Z. R. Dai, and Z. L. Wang, Science **291**, 1947 (2001).